Received: June 30, 2024. Revised: August 5, 2024.

INASS

International Journal of
Intelligent Engineering & Systems

http://www.inass.org/

Skin Cancer Classification Using Premature Convergence Strategy-based Artificial Jelly Search Optimization with Convolutional Neural Network

Usha Thirugnanam[1]* **Nalini Joseph[1]**

[1]*Department of Computer Science and Engineering,*
Bharath Institute of Higher Education and Research, Chennai, India
* Corresponding author's Email: t.ushausha@yahoo.com

Abstract: Melanoma, the deadliest type of skin cancer in humans, poses significant challenges while diagnosing skin lesions through thermoscopic imaging. These challenges include issues such as hair interference, inaccurate capturing of skin lesion shapes, and extraction of irrelevant features. However, overfitting occurs due to oversampling, resulting in erroneous skin cancer captures, and failure to detect noise and unwanted hair in melanoma images. The research proposes the Premature Convergence Strategy with Artificial Jelly Search Optimization (PCSAJSO) algorithm and Convolutional Neural Network (CNN) for classifying skin cancer into melanoma and non-melanoma. Initially, images are obtained from ISIC2018, ISIC2019, and PH2 datasets, used to analyze the performance of the proposed method. The W-Net method is utilized to segment skin cancer by capturing the contextual information from various scales in skin cancer images. The PCS technique ensures a balance between exploration and exploitation in search space which helps to increase convergence speed and adjusts population size for skin cancer classification. In comparison to the existing techniques like Inception-ResNet and U-Net, the PCSAJSO-CNN achieves commendable accuracies of 98.15%, 99.38%, 99.70%, 94.68%, and 97.08% respectively on the ISIC2016, ISIC2017, ISIC2018, ISIC2019 and PH2 datasets.

Keywords: Artificial jelly search optimization, Convolutional neural network, Premature convergence strategy, Skin cancer, W-Net.

1. Introduction

Skin cancer a widespread condition affecting individuals across all age groups that poses significant health risks and requires timely diagnosis and treatment. Early detection is crucial, as identifying the disease in its initial stages significantly improves treatment outcomes. [1, 2]. In 2018, melanoma affected both men and women, with 5,999 cases reported in men and 3,829 cases reported in women [3]. Detecting skin lesions presents a complex challenge due to several factors, including irregularities in capturing images of skin cancer and the occurrence of unwanted hair and noise [4]. The classification of skin cancer is complex due to the similarity between melanoma and non-melanoma lesions, resulting in a high degree of comparability within the disease [5]. Improving the survival rate significantly relies on effectively treating skin lesions. However, identifying lesions during inspection can be challenging, and the use of thermoscopic images assists in this process. [6].

The Deep Learning (DL) is used to segment and classify melanoma skin cancer, providing quality diagnostics for related diseases and improving patient care [7]. In the field of medical image recognition, neural networks are extensively involved in analysing skin cancer images, which often depict numerous small objects on human skin [8]. However, accurately locating small objects within the lesion region from normal skin is challenging due to the sophisticated differences in skin color, lesion location, and non-uniform lighting [9]. Implementing DL techniques and enhancing contrast for small melanoma objects has improved accuracy in trained models, effectively addressing the issue of imbalanced data that impacts the model's accuracy

[10]. This approach is essential for classifying skin lesions using deep learning techniques [11]. These structures are considered one of the primary keys for identifying and classifying melanoma or non-melanoma diseases [12]. CNNs face challenges in the classification of skin lesions, prompting the need for hyper-tuning phases. These phases optimize model parameters to efficiently provide accurate diagnoses in real-time to a specified criteria and enhance the performance in medical image analysis [13, 14]. Implementing the proposed approaches allows for the early detection of skin cancer, enabling more efficient treatment and reducing the associated mortality rate [15]. In this research, hyper parameter tuning process is integral to the classification performed by the Premature Convergence Strategy with Artificial Jelly Search Optimization (PCSAJSO). This optimization technique calculates the epochs, batch size and iterations based on the performance and then classifies melanoma and non-melanoma cases. The optimization technique aims to improve the search space and handle the convergence rate to ensure accurate parameter settings for skin cancer segmentation and classification models.

The main contributions of the research are written below:

- The PCS is a novel approach in skin cancer classification, expanding the search space and maximum convergence rate to improve the population size of hyper parameters for improvement.
- The CNNs possess a reduced parameter count compared to traditional neural networks, facilitating effective training of deep architectures with an optimized hyper parameter to accurately identify skin cancer.
- The PCSAJSO technique uses hyper parameter tuning for selecting appropriate values, combined with the CNN technique to improve the accuracy of classifying skin lesions as melanoma and non-melanoma.

The paper is organized as follows: Section 2 provides a literature review that summarizes skin cancer using DL techniques. Section 3 introduces the proposed method utilized by PCSAJSO-CNN. Section 4 discusses the result and comparative analysis, while Section 5 discusses the conclusion.

2. Literature review

To goal of skin lesion image segmentation is to extract and identify skin cancer. The relevant researches focused on the DL techniques for segmentation and classification of skin cancer are studied here.

Khouloud [16] presented a DL-based skin cancer segmentation approach involving W-net and ResNet Encoder-Decoder for classifying skin cancer diseases by using ISIC2016, ISIC2017 & ISIC2018 dataset. The segmentation process identified diseased areas based on shape and colour, facilitating disease analysis. The ResNet architecture captured the contextual information from different scales independently. However, the input image often contained noise and inaccuracies in capturing the skin lesion image, leading to difficulties in segmenting skin lesions.

Kaur [17] introduced a DL-based Convolutional Neural Network (CNN) framework for melanoma, an aggressive form of skin cancer by using ISIC2016, ISIC2017 & ISIC2018 dataset. The framework utilized a dilated convolutional network, leveraging atrous convolution in place of pooling layers. Atrous dilations were involved to expand the receptive field of the input vector without relying on pooling layers. The fixed-size filter slider served as the input feature, while the dilated CNN maintained spatial resolution and performed multiscale feature capture, thereby expanding the receptive field without introducing additional parameters. However, the network was heavy and consumed longer periods for execution due to numerous sampling and sampling layers.

Midasala [18] implemented an unsupervised learning (USL)-based K-means clustering (KMC) method for thresholding skin cancer regions in image segmentation by using ISIC2020 dataset. The USL-KMC approach involved thresholding skin lesion regions in images to segment skin cancer. This approach proved effective as clustering emerged as one of the most commonly used algorithms, reducing computational costs, executing faster, and simplicity, as opposed to other clustering methods. However, the clustering method caused the merging of lesions with the surrounding skin, while an abundance of clusters resulted in over-segmentation due to images with complex lesion shapes and overlapping segments.

Nawaz [19] developed a DL-based approach, DenseNet77-UNet which extracted segmentation power to identify small lesions by using ISIC2019, ISIC2020 dataset. While minimizing both training and testing skin diseases, even under noise and blurring due to the efficient computation of DenseNet77-UNet. The method calculated input sample computations, performed down sampling to reduce feature size, and attained the detailed image information. However, the performance of skin lesion region segmentation considerably decreased in low-resolution skin lesions and low-illumination conditions of images. This was attributed to the potential loss of essential features due to the

bottleneck technique, leading to poor convergence and overfitting.

Alsahafi [20] implemented a Residual Deep Convolutional Neural Network (RDCNN) for skin cancer segmentation by using ISIC2017, ISIC2018 dataset, which performed convolutional filtering for multi-layer feature extraction. This method directly processed raw image data, utilizing multiple filters to enhance the effectiveness of skin lesion categorization. However, under-sampling which removed samples from the majority class caused the loss of vital information for the model. Additionally, skin lesions occurring in a small range were difficult to be captured in skin cancer due to the rise of overfitting issues that necessitated a large amount of labelled data.

Nawaz [21] developed an automated system for the identification of melanoma skin cancer, addressing by using ISIC2017 & ISIC2018 dataset. Given the significant differences in mass structure and colour among skin lesions, they involved a Fuzzy K-means (FLM) clustering approach for segmentation. These methods effectively segmented skin lesion regions affected by skin cancer, delineating the apparent edges of the lesions and reducing the complexity of model training and testing. However, skin cancer diagnosis was often complicated by noise and blurring attacks, which further complicated the segmentation process, leading to challenges such as overlapping and reflecting complex data.

From the overall analysis, the existing techniques are seen to have limitations of inaccurate capturing of skin cancer, and failure to detect noise and unwanted hair in melanoma images. This research involves the PCSAJSO approach combined with CNN to address the optimization technique required to improve the accuracy of analysis of skin cancer images. Simultaneously, it aims to eliminate unwanted hair and noise from the images.

3. Proposed methodology

In this section, PCSAJSO and CNN methods are proposed for efficient classification of skin cancer, utilizing the datasets of ISIC2016, ISIC2017 ISIS2018, ISIC2019 & PH2. These datasets undergo pre-processing using the Gaussian Filter (GF) method and Dull Razor for the removal of hair, noise, marks, and stains, thereby improving the quality of the skin images. The pre-processed images are fed to segmentation for the skin lesion images by using W-net. The improvement involves capturing independent paths from different scales in a distinct manner.

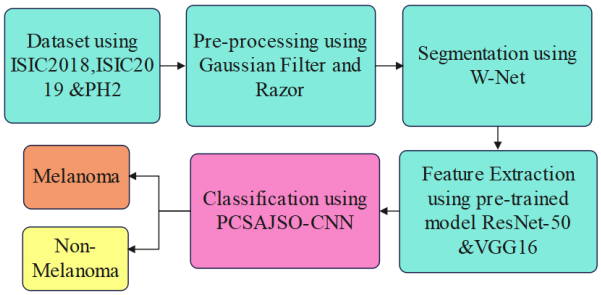

Figure. 1 Block diagram of the proposed method

The proposed method involves feature extraction using ResNet-50 and VGG-16, followed by the classification of melanoma and non-melanoma using Hyper Parameter Tuning techniques such as PCSAJSO, in combination with CNN methods. Fig. 1 shows the block diagram of the proposed method.

3.1 Dataset

The skin cancer datasets used in the research are International Skin Imaging Collaboration (ISIC) datasets from 2018 and 2019, along with the Pedro Hispano Hospital (PH2) dataset. These datasets collectively contain 21,063 thermoscopic images, collected for training and testing purposes. Below is a detailed explanation of three datasets. Fig. 2 shows the sample image of the ISIC2016, ISIC2017, ISIC2018, ISIC2019 & PH2 dataset.

3.1.1. ISIC 2016 & 2017 dataset

The ISIC 2016 [22] & 2017 [23] dataset consists of 2750 skin cancer image. The image consists of 2000 training dataset 150 test dataset and 600 validation datasets. High resolution of images in the ISIC 2016 & 2017 dataset provides an advantage over other dermoscopic image dataset. The DL model achieved high success in experimental settings, although it achieved moderate success in the clinical environment.

3.1.2. ISIC 2018 dataset

This section focuses on the ISIC 2018 dataset [24], which aims to classify lesion categories into several classes including, Dermatofibroma (Der), Nevus (Nev), Melanoma (Mel), Pigmented Benign (Pig-Be), Keratoses (Ker), Pigmented Bowen's (Pig-Bo), Vascular, and Basal Cell Carcinoma (BCC) [21]. The ISIC 2018 dataset comprises a total of 6296 images, with 2596 images allocated for training, 1002 for testing, 102 for validation, and 2596 for ground truth annotation.

Table 1. Dataset description ISIC 2019

Type of skin lesion	Training	Validation	Testing
Mel	360	3812	350
MN	965	1100	931
BCC	250	2820	253
AK	75	716	76
BK	203	2215	206
DF	1100	206	22
VL	24	202	27
SCC	42	541	45
Total image	1930	10523	1910

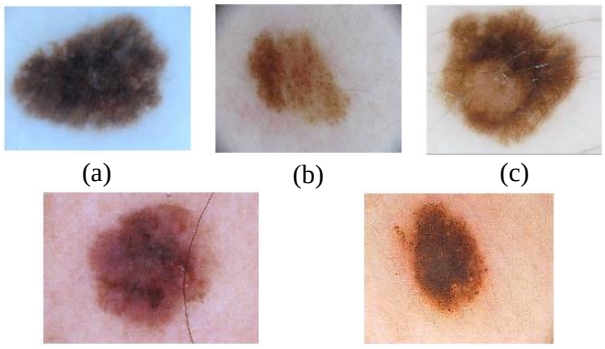

(a) (b) (c) (d) (e)

Figure. 2 Sample image of the ISIC2016, ISIC2017, ISIC2018, ISIC2019 & PH2 dataset: (a) ISIC2016 dataset, (b) ISIC2017 dataset, (c) ISIC2018 dataset, (d) ISIC2019 dataset, and (e)PH2 dataset

3.1.3. ISIC 2019 dataset

The ISIC2019 dataset [25] contains more than 14363 images classified into 8 skin diseases, enabling classification. The dataset is split into three sets of data with a split ratio of 0.8 for training, 0.1 for testing, and 0.1 for validation [22]. The eight categories include Melanoma (Mel), Melanocytic nevus, Basal Cell Carcinoma (BCC), Actinic Keratosis (AK), Benign keratosis (BK), Dermatofibroma (DF), Vascular Lesion (VL), and Squamous Cell Carcinoma (SCC). Below is the dataset description for ISIC 2019 presented in Table 1.

3.1.4. PH2 dataset

The PH2 dataset [26] comprises a total of 400 images from Pedro Hispano Hospital, divided into two classes: Nev and Mel. The training data are split into 200 instances, each for training x and training y. There are two classes: Nevus and Melanoma. The total number of images is 400.

3.2 Pre-processing

The collective dataset images serve as input for Pre-processing, where GF is involved to eliminate the irrelevant noise. This process aims to eliminate noise while preserving essential image features as much as possible. The wiener filter shows poor performance because it is challenging to accurately identify and isolate skin cancer region. In order to address this issue, the lesion part with noise is removed using GF, as numerically formulated in Eqs. (1) and (2).

$$h_g(n_1, n_2) = e^{\frac{-(n_1^2+n_2^2)}{2\sigma^2}} \tag{1}$$

$$h(n_1, n_2) = \frac{h_g(n_1,n_2)}{\sum_{n_1}\sum_{n_2} h_g} \tag{2}$$

In Eqs. (1) and (2), n_1 and n_2 represent the pixel values of the image, σ denotes the standard deviation, and h denotes the GF values. The Dull Razor is involved in removing hair from the skin during this process. Dull Razor computation is expressed by Eq. (3) below.

$$V_r(x,y) = 1, if\ K_t(x,y) > T \\ = 0, otherwise \tag{3}$$

The final phase for the original image is formed by aggregating three colour channels of the hair masks. This aggregation process is described by Eq. (4) below.

$$V = V_r \cup V_a \cup V_b \tag{4}$$

Refining the lesion points is a key stage in extracting functions for analysing and recognizing medical images. Techniques such as GF and the Dull Razor method are involved in noise removal and hair removal from medical images. These pre-processed images are then provided to the segmentation process for capturing lesion regions in skin cancer.

3.3 Segmentation

After the Pre-processing technique, the unwanted noise and hair is removed from the image. The goal of segmentation is a process of identifying lesion regions within the skin and distinguishing them to identify skin cancer. In this research, segmentation involves a new DL architecture called W-Net. This architecture focuses on dual-path semantics lesion region and aims to accurately extract skin cancer images by utilizing two mutually independent paths to capture contextual information at different scales. During up-sampling, bilinear interpolation is involved to reduce feature map distortion and integrate the differently processed skin images. W-Net utilizes ResNet blocks and convolutional blocks

(a) (b) (c)

Figure. 3 Sample segmented image:
(a) ISIC2018, (b) ISIC2019, and (c) PH2 dataset

for both down-sampling and up-sampling processes.

The W-Net encoder generates input codes from raw skin images using an auto encoder architecture for segmentation.

This process involves two steps with the decoder layer matching the number of encoder layers. The ResNet block functions as a residual unit, featuring two convolutional blocks that identify mapping. The convolutional network design follows throughout the down sampling path, with two $3x3$ convolutions. Skin regions are segmented for training and testing, with image cropping performed after manual segmentation to eliminate irrelevant details. Network performance is assessed using the Dice coefficient index. Attention mechanisms are integrated into the ResNet structure to address variations in lesion size and shape, thereby enhancing the network performance through suppression of feature activations. The concatenation between ResNet decoder and ConvNet encoder focuses on skin lesion regions of interest, allowing for better segmentation. The segmented skin lesion image is provided for feature extraction. Fig. 3 represents the sample segmented image.

3.4 Feature extraction

After tumor segmentation, capturing the boundary region of the tumor aids in the detection of skin cancer. The goal of the feature extraction method is to extract several beneficial feature vectors in skin cancer. Pre-trained models such as ResNet-50 and VGG-16 are involved for this purpose, which are then adapted for global classification performance. ResNet-50 trains the data efficiently without the trained data encountering the vanishing gradient problem, allowing it to handle complex tasks and extract intricate features from data. It has been applied to a wide range of melanoma skin cancer cases, achieving impressive accuracy in classifying skin lesions. In skin cancer analysis, VGG-16's simplicity and effectiveness contribute to strong performance in skin cancer classification tasks, with convolutional layers followed by max-pooling layers progressively increasing in depth.

3.4.1. ResNet 50

The ResNet-50-layer residual network's increased accuracy comes at the cost of higher computational resources. Training and inference with this model demand more memory and processing power. Due to its depth and complexity, ResNet-50 requires longer training time when compared to lightweight architectures [13]. In this research, it is necessary to consider this trade-off when choosing a model. Adapting deeper networks is advantageous for deep learning methods, and in this case, networks with 20-30 layers are utilized. The residual units allow the training of a 152-layer model, which performs well on the data. There is a shallower learning curve due to the novel residual structure.

3.4.2. VGG 16

The VGG-16 architecture involves taking weights and parameters learned from the existing VGG-16 models and applying them to create new models better suited for skin cancer [13]. This approach helps achieve better results with VGG16 models while using fewer resources. Pre-trained networks like VGG-16 that have already been trained on skin cancer image datasets, are fine-tuned by adding additional layers and adjusting some hyper parameters to make them suitable for this model. The features extracted are given as input to hyper parameter tuning using PCSAJSO with CNN classification for skin lesions.

3.5 Image classification

After feature extraction, the purpose of this research is to automatically diagnose melanoma using CNN, a DL technique. CNNs are utilized to collect sophisticated convolutional filters and analyse various picture structures in skin cancer. The feature extraction process aims to accurately distinguish across distinct classes. However, there is always the risk of inadequate description when using a limited range of traits. Hyper parameter tuning using PCSAJSO is then involved in classifying melanoma and non-melanoma cases.

3.5.1. Hyper parameter tuning using AJSO algorithm

Hyper parameter tuning is the process of optimizing the parameters that during the training data and hyper parameter tuning, are needed, so as to select appropriate values and improve the model's performance by increasing accuracy. In this research, hyper parameter tuning using JSO and optimizing hyper parameters effectively enhance the

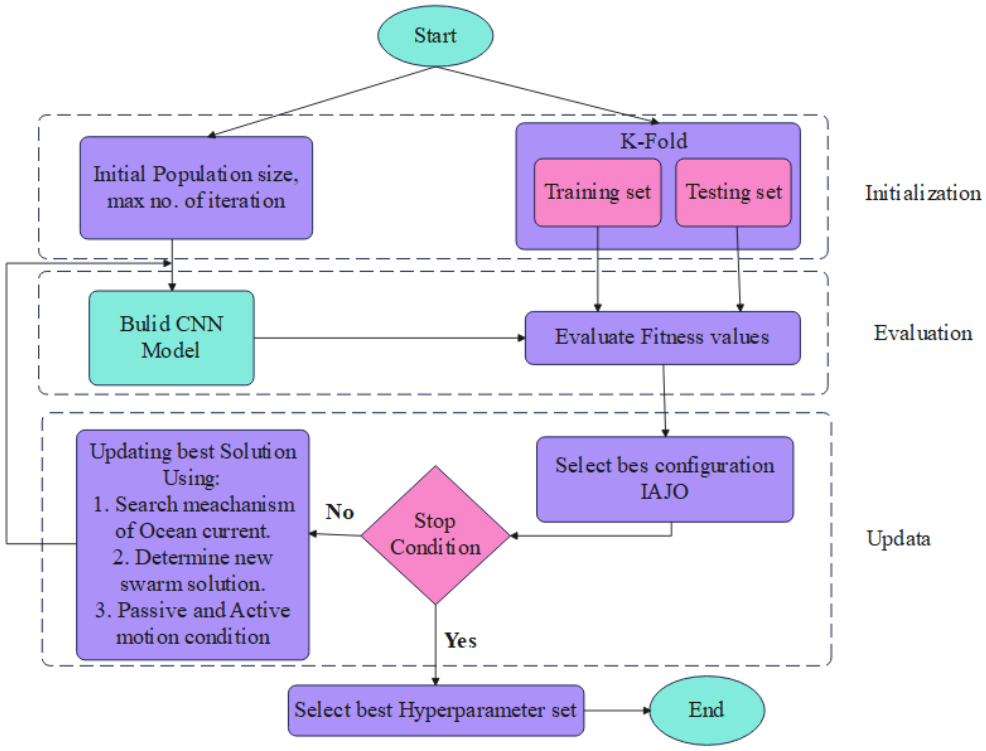

Figure. 4 Overall process of classification

performance of the classification model for skin cancer. The optimization technique in skin cancer involves finding its optimal solution using a powerful algorithm such as the AJSO algorithm.

The jellyfish, found in the sea, adapts to varying temperatures and pressures. The AJSO algorithm consists of three phases as described below:

- The jellyfish navigates the ocean currents, moving towards other jellyfish to coordinate their movements and reach their destination efficiently.
- In search of food, the jellyfish wander through the water, occupying areas where food is available.
- Once they find food, they stay there despite some hardship. Various activities are performed to search for food and determine the locations of large food sources. Fig. 4 illustrates the overall process of classification.

A detailed description of the parameters for the optimization method is provided below: The smoothing parameter σ is initially assigned randomly, where optimization techniques require solution encoding. In this solution encoding, a jellyfish analogy is used for each parameter, represented by M. The objective of the solution encoding procedure calculates the fitness function for improving the classification accuracy. After fitness computation, a significant number of ocean currents present in the jellyfish are attracted to areas at high levels. To exhibit behaviours resembling ocean currents and navigate within the swarm, the ability to transition between behaviours is timed-based. Additionally, the chaotic map is involved alongside more standard random methods for initialization to optimize the strategy in low search spaces and mitigate local minimum occurrences in the AJSO. The logistic map is mathematically represented by Eq. (5).

$$\overrightarrow{M_{n+1}} = \eta\overrightarrow{M_n}(1 - M_n), 0 \le \overrightarrow{M_0} \le 1 \quad (5)$$

Where, $\overrightarrow{M_n}$ denotes the vector of chaotic logistic values of the jellyfish. The initial values of the jellyfish are $\overrightarrow{M_0}$. The jellyfish are generated using the fitness function Eq. (4) to achieve maximum accuracy. The current position of each jellyfish is updated using the time-controlled mechanism. The swarm strategy involves swimming with the ocean currents and navigating inside the swarm. The mathematical description of the ocean circulation is given by Eq. (6).

$$\overrightarrow{M_n}(\mathrm{t}+1) = \overrightarrow{M_n}(t) + \vec{r}.*\left(\overrightarrow{M^*}\beta * r_1 * \mu\right) \quad (6)$$

The variable r is a random vector that occurs between 0 and 1, and each component of the vector is

denoted by a dot. The variable m denotes the population, and r is a random integer used for access. There are two types of moments: active and passive, as mathematically expressed in Eq. (7).

$$\overrightarrow{M_n}(\mathrm{t}+1) = \overrightarrow{M_n}(t) + \overrightarrow{r_3} * \gamma * (U_b - L_b) \quad (7)$$

Where, the random integer r is assigned a value of 3, indicating that the distance travelled in a circle centered on the current location is greater than 0. The search space is denoted by the upper and lower bounds, denoted as U_b and U_l respectively. The dynamic motion is represented by Eq. (8).

$$\overrightarrow{M_n}(\mathrm{t}+1) = \overrightarrow{M_n}(t) + \vec{r} * \vec{D} \quad (8)$$

Where, a random number vector ranging from 0 to 1 is used for the current jellyfish generation. The movement for food search is calculated using the following Eq. (9).

$$\vec{D} = \begin{cases} \overrightarrow{M_n}(t) - \overrightarrow{M_m}(t), if\ f(\overrightarrow{M_n}) < f(\overrightarrow{M_m}) \\ \overrightarrow{M_n}(t) - \overrightarrow{M_m}(t), \quad otherwise \end{cases} \quad (9)$$

The randomly chosen jellyfish is indexed as m, and f represents the fitness function. Time control is considered in the function given by Eq. (10).

$$c(t) = \left(1 - \frac{t}{t_{max}}\right) * (2 * r - 1) \quad (10)$$

Where, the current evaluation is denoted as $(r, 0)$, where r is an integer, and s represents the greatest evaluation. The jellyfish swim with the ocean current, exhibiting both active and passive motions within the swarm, depending on a randomly generated integer between 0 and 1.

3.5.2. Proposed premature convergence strategy artificial jellyfish search optimization

The JSO is combined to form a new approach that more efficiently controls variables between exploitation methods, aiding in the detection of skin cancer images and avoiding local minima. The initialization provides a population of n solutions, where d is the number of dimensions. After involving the chaotic logistic map from section 3.5.1, the region to be detected undergoes local exploration to enhance the capability of searching for the skin cancer images. The improved AJSO is utilized to classify melanoma and non-melanoma. The improved technique using the PCS is performed in the large search space to provide classified skin images. The PCS technique is represented by Eq. (11).

$$\overrightarrow{M_n}(\mathrm{t}+1) = \overrightarrow{M_n}(t) + \vec{r} * \left(\overrightarrow{M_{r1}}(\mathrm{t}) - \overrightarrow{M_{r2}}(\mathrm{t})\right) + (1 - \mathrm{r}) * \left(\mathrm{M}^{*} - \overrightarrow{M_{r3}}(\mathrm{t})\right) \quad (11)$$

The parameter r is used with values 1, 2, and 3 in the random solution to perform skin cancer prediction, layering the image to classify and validate the cancer images. The AJO algorithm is initialized with PCA reduced set of features and updated positions of jellyfish, with iteration until the optimal set of features and hyper parameters are found. The population size is increased in PCS to involve skin cancers with many available classes, training for each type of skin cancer, and using the increased size to transfer CNN. The control parameter is set low to move closer to the best solution, speeding up convergence, while a high value updates the current solution. In this research, PCA combined with AJSO strategy, where the efficiency is improved to find optimal solutions with minimal resource consumption.

3.5.2. Convolutional neural network

The hyper parameter tuning provided to CNNs is built to incorporate spatial structure inputs, originally inspired by the visual system of human skin. Hyper parameter tuning aims to maximize the efficiency of computational resources. Without hyper parameter, the skin cancer classification process uses default parameter values for the CNN model, leading to suboptimal performance and reduced efficiency. Hyper parameter tuning is necessary because selecting appropriate values improves the accuracy of skin cancer classification. CNNs possess a reduced parameter count, when compared to traditional neural networks, facilitating effective training of deep architectures comprising more than 5 layers, particularly in tasks of skin cancer analysis, where fully connected networks struggle to perform efficiently. The CNN comprises input layers, output layers, and several hidden layers, including convolutional ReLU pooling, fully connected, and normalization layers. At each iteration of training, accuracy is enhanced utilizing the optimized technique, followed by a reduction in training accuracy occurs. This process is plotted over multiple iterations. The model is trained for 30 epochs with a batch size of 32 and a dropout layer of 0.4 to avoid overfitting. The validation loss is monitored for 30 epochs. Table 2 represents the Hypermeter tuning ranges.

The accuracy of the model obtained is 99.63% and ReLU activation function is used for training as in Eq. (12).

$$y = \max(0, n) \tag{12}$$

The ReLU is an interesting transformation that activates a node only if the input is above a certain threshold. When the input is below zero, the output remains zero, but as soon as the input rises above a certain threshold, the relationship becomes linear, with the dependent variable $f(x) = \max(0, n)$. The softmax function is another function used to transform output values from the model into a probability distribution. The softmax function is defined by Eq. (13).

$$\sigma(\vec{Y})_i = \frac{e^{Y_i}}{\sum_{j=1}^{V} e^{Y_i}} \tag{13}$$

Where, σ is indicated the softmax and input vector is $\vec{Y}$, an extensive analysis of skin cancer comparing various CNN architectures reveals that the ResNet-50 architecture outperforms others, offering superior performance with minimal computational demands. In this study, the variability in data is comparatively lower than in other skin lesion classifications, rendering CNNs highly efficient for real-time diagnosis. The chosen model strikes a balanced compromise between speed and accuracy, making it an optimal choice for the research at hand.

4. Experimental Results

The proposed network PCSAJSO with CNN is trained on a two-year dataset comprising (ISIC2016, ISIC2017, ISIC2018 & ISIC2019) and the PH2 dataset to illustrate the effectiveness of the suggested DL technique compared to other existing methods. The implementation of the proposed method is carried out using MATLAB R2020a and the required system configuration includes an i6 processor, 16 GB of RAM, and Windows 10 Operating System. The performance measures used for evaluation and the results of the classification are explained as follows. The parameter metrics are defined by Eqs. (14) to (19).

$$Accuracy = \frac{(TP+TN)}{(TP+TN+FP+FN)} \tag{14}$$

$$Precision = \frac{TP}{(TP+FP)} \tag{15}$$

$$Specificity = \frac{TP}{(TN+FP)} \tag{16}$$

$$Sensitivity = \frac{TP}{(TP+FN)} \tag{17}$$

$$JAC = \frac{TP}{TP+FP+FN} \tag{18}$$

$$DICE = \frac{2*TP}{2*TP+FP+FN} \tag{19}$$

Where TP, TN, FP, and FN respectively denote True Positive, True Negative, False Positive, and False Negatives. The proposed method involves classification using hyper parameter tuning PCAAJO algorithm with CNN methods, providing high classification performance.

4.1 Performance analysis

In this section, the performance of the classification process is evaluated using various performance metrics of Accuracy, Precision, Specificity, Sensitivity, Jaccard Index (JAC), and Dice on the ISIC2016, ISIC2017, ISIC 2018, ISIC 2019, and PH2 datasets. The classification involves hyper parameter tuning using the optimization PCSAJSO algorithm combined with CNN methods. The hyper parameter configuration is used to train the network end-to-end. The segmentation process with the dataset is represented in Table 3. The classification process with datasets is displayed in tables 5 to 7, which describe the classification results.

Table 3. Segmentation result

Datasets	Methods	JAC	DICE
ISIC2017	ANN	0.9284	0.9472
	CapNet	0.9375	0.9536
	RNN	0.9425	0.9672
	DNN	0.9563	0.9715
	W-Net	0.9690	0.9815
ISIC2018	ANN	0.9345	0.9425
	CapNet	0.9455	0.9535
	RNN	0.9565	0.9645
	DNN	0.9674	0.9756
	W-Net	0.9776	0.9875
ISIC2019	ANN	0.9345	0.9425
	CapNet	0.9455	0.9545
	RNN	0.9565	0.9655
	DNN	0.9674	0.9768
	W-Net	0.9776	0.9878
PH2	ANN	0.9325	0.9425
	CapNet	0.9454	0.9545
	RNN	0.9565	0.9655
	DNN	0.9672	0.9768
	W-Net	0.9779	0.9878

The performance of the W-Net segmentation method is evaluated based on JAC and DICE on the ISIC2016, ISIC2017, ISIC 2018, ISIC 2019 and PH2 dataset, as described in Table 4. The existing methods using classification techniques such as Recurrent Neural Network (RNN), and Deep Neural Network (DNN) are evaluated. The W-Net method achieves a high JAC of 0.9774 and DICE of 0.9875. The classification technique is W-Net which achieves a high JAC, reaching 99.70% because it accurately captures the skin lesion region.

The performance of the CNN classification method is evaluated based on accuracy, precision, specificity, sensitivity, on the ISIC 2018 dataset, as described in Table 4. The existing methods using classification techniques such as RNN, and DNN, are evaluated. The CNN method achieves a high accuracy of 99.70%, specificity of 99.38%, sensitivity of 99.48%, and precision of 98.55%. The classification technique CNN achieves a superior accuracy, reaching up to 99.70%, because it accurately captures the skin lesion region and then classifies melanoma and non-melanoma cases.

The ISIC 2019 dataset using CNN method achieves a high accuracy of 94.68%, specificity of 96.80%, sensitivity of 93.81%, and precision of 94.58%. The classification technique CNN attains high specificity, reaching 96.80% because its specificity is referred to as the segmented proportion of non-lesion regions. The PH2 dataset using CNN method attains a high accuracy of 98.08%, specificity of 99.0%, sensitivity of 99.51%, and precision of 99.54%. The classification using the CNN technique attains a commendable accuracy of 99.54%, due to its precision in accurately predicting the ratio of positive observations.

Table 4. Performance analysis of classification method

Datasets	Methods	Accuracy (%)	Precision (%)	Specificity (%)	Sensitivity (%)
ISIC 2017	RNN	97.45	97.25	96.83	96.35
	DNN	98.52	98.14	97.26	97.83
	CNN	**99.38**	**99.70**	**98.78**	98.12
ISIC2018	RNN	97.65	96.35	97.20	97.25
	DNN	98.69	97.45	98.25	98.35
	CNN	**99.70**	**98.55**	**99.38**	**99.48**
ISIC2019	RNN	92.50	92.45	92.25	91.72
	DNN	93.60	93.50	95.75	92.77
	CNN	**94.68**	**94.58**	**96.80**	**93.81**
PH2	RNN	96.99	97.25	97.98	97.15
	DNN	97.01	98.45	98.01	98.45
	CNN	**98.08**	**99.54**	**99.05**	**99.51**

4.2 Comparative analysis

The performance of the proposed PCSAJO-CNN method is contrasted against the existing methods including Inception ResNet [16], V-Net 2D, ResNet 2D [17], U-Net with DenseNet 77 [19], RDCNN [20], and FKM [21]. The comparative analysis involves three datasets: ISIC2016, ISIC2017, ISIC 2018, ISIC 2019, and PH2. In this research, the proposed PCSAJO-CNN method attains a superior accuracy of 98.15% on the ISIC 2016, 99.38% accuracy on the ISIC 2017, 99.70% accuracy on the ISIC 2018 dataset, 94.68% accuracy on the ISIC 2019 dataset, and 97.08% accuracy on the PH2 dataset. Table 5 displays the comparative analysis of the proposed method for classification.

Table 5. Comparative analysis of the proposed method for classification

Dataset	Methods	Accuracy (%)	Precision (%)	Specificity (%)	Sensitivity (%)	JAC (%)	DICE (%)
ISIC2016	W-Net – Inception Resnet [16]	98.01	98.1	98.1	98.1	N/A	N/A
	Proposed PCSAJSO-CNN method	**98.15**	**98.17**	**98.10**	**98.09**	**0.9854**	**0.9542**
ISIC2017	W-Net – Inception Resnet [16]	96.97	95.71	97.81	95.15	N/A	N/A
	CNN [17]	N/A	N/A	N/A	N/A	0.818	0.884
	RDCNN [20]	99.21	99.66	98.73	N/A	0.9688	0.9802
	FLM [21]	99.32	N/A	N/A	N/A	N/A	N/A
	Proposed PCSAJSO-CNN method	**99.38**	**99.70**	**98.78**	**98.12**	**0.9690**	**0.9815**
ISIC2018	U-Net with Densenet 77 [19]	99.51	N/A	99.35	99.44	0.9771	0.9873
	RDCNN [20]	N/A	N/A	N/A	N/A	0.9688	0.9873
	FKM [21]	99.63	N/A	N/A	N/A	N/A	N/A
	Proposed PCSAJSO-CNN method	**99.70**	**98.55**	**99.38**	**99.48**	**0.9775**	**0.9878**
ISIC2019	RDCNN [20]	94.65	72.56	96.78	70.78	N/A	N/A
	Proposed PCSAJSO -CNN method	**94.68**	**94.58**	**96.80**	**93.81**	**0.9256**	**0.9125**
PH2	W-Net – Inception Resnet [16]	97.5	98.50	99.00	N/A	N/A	N/A
	Proposed PCSAJSO -CNN method	**98.08**	**99.54**	**99.05**	**99.51**	**0.9125**	**0.9236**

5. Discussion

In this section, the advantage of the proposed method and the limitations of existing method are discussed. The existing methods have certain limitations like: The W-Net Inception [16] input image often contains noise, leading to inaccurate segmentation and a lack of capture of the skin lesion image, thereby making segmenting specific object categories challenging. The DenseNet 77-U-Net [19] method for skin lesion region segmentation significantly decreases in low-resolution and low-illumination images. Additionally, the potential loss of essential features due to the bottleneck technique causing poor convergence and overfitting. The RDCNN [20] method struggles to capture skin lesions occurring in a small range, making it challenging to detect skin cancer. This is due to overfitting issues and the necessity for a large amount of labeled data. FKM [21] performs skin cancer classification relatively slowly, as accessing centroids in the image is not efficient and data points are not constrained to clusters. In this research, hyperparameter tuning using IAJSO with CNN enhances the model's spatial capabilities and focuses on relevant skin cancer classification. This approach successfully avoids overfitting and improves accuracy.

6. Conclusion

In this research, PCSAJSO combined with CNN is suggested for the classification process to extract the affected areas in skin cancer images. However, overfitting occurs in skin cancer images where the convergence rates are low, resulting in inefficient classification of melanoma and non-melanoma images. The gathered images undergo pre-processing utilizing a Gaussian Filter to eliminate noise which are then subjected to the removal of unwanted hair using a dull razor. The input images are fed into W-Net for segmentation of skin lesion regions with manual segmentation followed by image cropping to remove irrelevant details. Feature extraction is performed using pre-trained models such as ResNet-50 and VGG-16, which are adapted for an efficacious global classification performance. Moreover, the hyperparameter tuning using the PCSAJSO algorithm with CNN improves the maximum accuracy to efficiently capture melanoma skin images and avoid overfitting through optimization techniques. In comparison to the existing techniques like Inception-ResNet and U-Net, the PCSAJSO-CNN achieves commendable accuracies of 99.38%, 99.70%, 94.68%, and 97.08% respectively on the ISIC2017, ISIC2018, ISIC2019 and PH2 datasets. In the future work, hybrid techniques in skin cancer classification will leverage the complementary strengths of traditional methods and deep learning to enhance feature selection, interpretability, data efficiency, and generalization.

Notation

Notation	Description
n_1 and n_2	Pixel value of image
σ	Standard deviation
h	Gaussian values
$\overrightarrow{M_n}$	Vector of chaotic logistic value
$\overrightarrow{M_0}$	Initial values
r	Random vector
U_b and U_l	Upper and lower bounds
r, s	Integer, greatest evaluation
$f(x) = \max(0, n)$	Linear dependent variable
$\sigma, \vec{Y}$s	Softmax and input vector

Conflicts of Interest

The authors declare no conflict of interest.

Author Contributions

The paper conceptualization, methodology, software, validation, formal analysis, investigation, resources, data curation, writing—original draft preparation, writing—review and editing, visualization, have been done by 1st author. The supervision and project administration, have been done by 2nd, and 3rd author.

References

[1] V. Radhika, and B.S. Chandana, "Effective Deep Learning Network Model for Multi-Class Skin Cancer Classification", *International Journal of Intelligent Engineering & Systems*, Vol. 16, No. 6, pp. 771-782, 2023, doi: 10.22266/ijies2023.1231.64.

[2] A. Alhudhaif, H. Ocal, N. Barışçı, I. Atacak, M. Nour, and K. Polat, "A novel approach to skin lesion segmentation: Multipath fusion model with fusion loss", *Computational and Mathematical Methods in Medicine*, Vol. 2022, p. 2157322, 2022.

[3] M.A. Khan, M.I. Sharif, M. Raza, A. Anjum, T. Saba, and S.A. Shad, "Skin lesion segmentation and classification: A unified framework of deep neural network features fusion and selection", *Expert Systems*, Vol. 39, No. 7, p. e12497, 2022.

[4] S. Din, O. Mourad, and E. Serpedin, "LSCS-Net: A lightweight skin cancer segmentation

network with densely connected multi-rate atrous convolution", *Computers in Biology and Medicine*, Vol. 173, p. 108303, 2024.

[5] N. ul Huda, R. Amin, S.I. Gillani, M. Hussain, A. Ahmed, and H. Aldabbas, "Skin cancer malignancy classification and segmentation using machine learning algorithms", *JOM*, Vol. 75, No. 8, pp. 3121-3135, 2023

[6] A. Bindhu, and K.K. Thanammal, "Segmentation of skin cancer using Fuzzy U-network via deep learning", *Measurement: Sensors*, Vol. 26, p. 100677, 2023.

[7] K. Aljohani, and T. Turki, "Automatic classification of melanoma skin cancer with deep convolutional neural networks", *AI*, Vol. 3, No. 2, pp. 512-525, 2022.

[8] C. Xin, Z. Liu, K. Zhao, L. Miao, Y. Ma, X. Zhu, Q. Zhou, S. Wang, L. Li, F. Yang, S. Xu, and H. Chen, "An improved transformer network for skin cancer classification", *Computers in Biology and Medicine*, Vol. 149, p. 105939, 2022.

[9] P. Chen, S. Huang, and Q. Yue, "Skin lesion segmentation using recurrent attentional convolutional networks", *IEEE Access*, Vol. 10, pp. 94007-94018, 2022.

[10] K. Mridha, M.M. Uddin, J. Shin, S. Khadka, and M.F. Mridha, "An interpretable skin cancer classification using optimized convolutional neural network for a smart healthcare system", *IEEE Access*, Vol. 11, pp. 41003-41018, 2023.

[11] H.L. Gururaj, N. Manju, A. Nagarjun, V.N.M. Aradhya, and F. Flammini, "DeepSkin: a deep learning approach for skin cancer classification", *IEEE Access*, Vol. 11, pp. 50205-50214, 2023.

[12] S. Mustafa, M.W. Iqbal, T.A. Rana, A. Jaffar, M. Shiraz, M. Arif, and S.A. Chelloug, "Entropy and Gaussian Filter-Based Adaptive Active Contour for Segmentation of Skin Lesions", *Computational Intelligence and Neuroscience*, 2022.

[13] W. Salma, and A.S. Eltrass, "Automated deep learning approach for classification of malignant melanoma and benign skin lesions", *Multimedia Tools and Applications*, Vol. 81, No. 22, pp. 32643-32660, 2022.

[14] S. Venkatasubramanian, A. Suhasini, and C. Vennila, "Improved Jellyfish Search Algorithm based Multipath Routing with Atom Search Algorithm for Best CH Selection", *Mathematical Statistician and Engineering Applications*, Vol. 71, No. 4, pp. 7389-7411, 2022.

[15] A. Magdy, H. Hussein, R.F. Abdel-Kader, and K.A.E. Salam, "Performance Enhancement of Skin Cancer Classification using Computer Vision", *IEEE Access*, Vol. 11, pp. 72120-72133, 2023.

[16] S. Khouloud, M. Ahlem, T. Fadel, and S. Amel, "W-net and inception residual network for skin lesion segmentation and classification", *Applied Intelligence*, Vol. 52, No. 4, pp. 3976-3994, 2022.

[17] R. Kaur, H. GholamHosseini, R. Sinha, and M. Lindén, "Automatic lesion segmentation using atrous convolutional deep neural networks in dermoscopic skin cancer images", *BMC Medical Imaging*, Vol. 22, No. 1, p. 103, 2022.

[18] V.D. Midasala, B. Prabhakar, J.K. Chaitanya, D. Sirnivas, D. Eshwar, and P.M. Kumar, "MFEUsLNet: Skin cancer detection and classification using integrated AI with multilevel feature extraction-based unsupervised learning", *Engineering Science and Technology, an International Journal*, Vol. 51, p. 101632, 2024.

[19] M. Nawaz, T. Nazir, M. Masood, F. Ali, M.A. Khan, U. Tariq, N. Sahar, and R. Damaševičius, "Melanoma segmentation: A framework of improved DenseNet77 and UNET convolutional neural network", *International Journal of Imaging Systems and Technology*, Vol. 32, No. 6, pp. 2137-2153, 2022.

[20] Y.S. Alsahafi, M.A. Kassem, and K.M. Hosny, "Skin-Net: A novel deep residual network for skin lesions classification using multilevel feature extraction and cross-channel correlation with detection of outlier", *Journal of Big Data*, Vol. 10, No. 1, p. 105, 2023.

[21] M. Nawaz, T. Nazir, M.A. Khan, M. Alhaisoni, J.Y. Kim, and Y. Nam, "MSeg-Net: a melanoma mole segmentation network using CornerNet and fuzzy K-means clustering", *Computational and Mathematical Methods in Medicine*, Vol. 2022, p. 7502504, 2022.

[22] ISIC2016 Dataset: https://www.kaggle.com/datasets/afrozaakter1604004/isic2016 (Accessed April 2024).

[23] ISIC2017 Dataset: https://www.kaggle.com/datasets/sarahmasdeh/isic2017 (Accessed on April 2014).

[24] ISIC2018 Dataset: https://www.kaggle.com/datasets/xxc025/isic2018 (Accessed on April 2024).

[25] ISIC2019 Dataset: https://www.kaggle.com/datasets/bhanuprasanna/isic-2019 (Accessed on April 2024).

[26] PH2 Dataset: https://www.kaggle.com/datasets/athina123/ph2dataset (Accessed on April 2024).